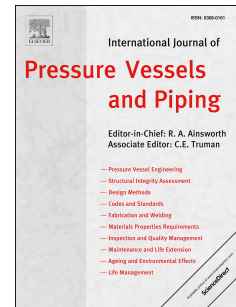


Journal Pre-proof

Creep damage analysis of mod.9Cr–1Mo steel welds considering void mechanics modeling

Takashi Honda, Takuya Fukahori, Takumi Tokiyoshi, Yasuharu Chuman, Toshihide Igari, Alan CF. Cocks



PII: S0308-0161(20)30226-X

DOI: <https://doi.org/10.1016/j.ijpvp.2020.104251>

Reference: IPVP 104251

To appear in: *International Journal of Pressure Vessels and Piping*

Received Date: 26 April 2020

Revised Date: 30 October 2020

Accepted Date: 10 November 2020

Please cite this article as: Honda T, Fukahori T, Tokiyoshi T, Chuman Y, Igari T, Cocks AC, Creep damage analysis of mod.9Cr–1Mo steel welds considering void mechanics modeling, *International Journal of Pressure Vessels and Piping* (2020), doi: <https://doi.org/10.1016/j.ijpvp.2020.104251>.

This is a PDF file of an article that has undergone enhancements after acceptance, such as the addition of a cover page and metadata, and formatting for readability, but it is not yet the definitive version of record. This version will undergo additional copyediting, typesetting and review before it is published in its final form, but we are providing this version to give early visibility of the article. Please note that, during the production process, errors may be discovered which could affect the content, and all legal disclaimers that apply to the journal pertain.

© 2020 Published by Elsevier Ltd.

T. Honda: Conceptualization, Methodology
T. Fukahori: Writing original draft
T. Tokiyoshi: Resources, Visualization
Y. Chuman: Project administration
T. Igari: Supervision
ACF Cocks: Writing-Reviewing and Editing

Creep Damage Analysis of Mod.9Cr-1Mo Steel Welds Considering Void Mechanics Modeling

Takashi Honda ^{*}, Takuya Fukahori ^{*}, Takumi Tokiyoshi ^{*}, Yasuharu Chuman ^{*}, Toshihide Igari ^{*} and Alan CF Cocks ^{**}

^{*} Research and Innovation Center, Mitsubishi Heavy Industries, LTD., 5-717-1, Fukahori-machi, Nagasaki, Japan

^{**}Department of Engineering Science, University of Oxford, Parks Road, Oxford, UK

Corresponding author (E-mail): Takashi Honda (takashi3_honda@mhi.co.jp)

Abstract

Since creep strength reduction of mod.9Cr-1Mo steel welds in long-term creep was confirmed experimentally, residual life prediction for Type IV creep failure has been an important theme in Ultra Super Critical (USC) plants after long-term service. The mechanism of Type IV creep failure within the fine-grained heat affected zone (FGHAZ) is twofold; an increase in number density of creep voids of a size comparable to FGHAZ grain size (5 μ m), and strain softening in the last stage of creep life. In this paper, a creep damage analysis scheme considering the above two mechanisms is applied to welded joints with non-uniform weld metal materials, heat affected zone (HAZ) and base metal, such as those found in large uniaxial cross-weld specimens. A void mechanics model expresses the increase of number density of creep voids (creep void density) in terms of a strain for void nucleation, which is strongly influenced by the multiaxial state of stress. A critical value of creep void density corresponding to the initiation of a micro-crack is determined based on the results of a random-fracture-resistance model of grain boundaries by the authors of this paper. Both the creep void density distribution and the failure process with crack initiation, propagation and final rupture predicted by the analysis are compared with experimental results at 650°C.

Key words: Creep, Creep cavity, Creep void, Type IV, Modified 9Cr-1Mo steel, Welded joints, Damage mechanics

1. Introduction

High chromium steels such as modified 9Cr-1Mo steel (ASME P91) with excellent creep strength are used in power piping such as the main steam pipes in USC (ultra-supercritical) power plants. Creep strength of welded joints, such as similar and dissimilar metal welds, is a key to confirming structural reliability in long-term operation. Both Type IV creep failure [1, 2] in similar metal welds

and interface failure [3, 4] in dissimilar metal welds of P91/Inconel are considered in the design stage and residual life prediction at high temperatures. Since creep strength reduction in similar metal welds of mod.9Cr-1Mo steel was experimentally confirmed in long-term creep tests [5], residual life predictions for Type IV creep failure have also been an important issue in USC plants during long-term service. There has been a major global effort to understand, quantify and prevent Type IV failure [1, 2]. Type IV creep failure is found in the FGHAZ (fine-grained heat affected zone), whereby nucleation, growth and coalescence of creep voids form micro-cracks. To avoid this failure mode in newly fabricated plants, a new design-allowable stress which reflects long-term creep data of welded joints is necessary; a residual life prediction method, however, is required for plants currently in operation. In addition to longitudinal welds subject to internal pressure, circumferential welds subject to internal pressure and bending are also considered [6, 7].

From a metallurgical point of view [8], the high-creep strength of mod.9Cr-1Mo steel is due to the introduction of various strengthening mechanisms against creep deformation. However, these mechanisms are gradually diminished due to microstructural changes during long-term creep, such as a decrease in the number density of precipitates ($M_{23}C_6$ etc.) accompanying an increase in their size; and an increase in the size of lath-martensitic microstructures. During the welding process of mod.9Cr-1Mo steel, a HAZ is created between weld metal and base metal. As a result of the welding process and subsequent PWHT, the edge of the HAZ adjacent to the base metal, known as the FGHAZ, develops an equiaxial fine-grained structure with low hardness and low creep strength.

Nucleation process of void is generally influenced by microstructure and chemical compositions [9]. Masuyama et al. [10] carried out microscopic observation of nucleation process in FGHAZ of welded joint specimen, using KA-SCMV28 (SA-387 Gr.91) fabricated material in Japan. This is the same material which is used in the experiment of welded joint by Komai et al. [11]. This material is equivalent to SA-387 Gr.91 Type 2 (Class 2) and amount of impurity elements such as S, Cu, Sn, As and Sb is low.

According to the microscopic observation of the nucleation process of creep voids in the FGHAZ of modified 9Cr-1Mo steel by Masuyama et al. [10], creep cavities of submicron size nucleate at precipitates, at triple points, or grain boundaries of 5 μ m-size grains, after which they grow and coalesce. They then surround the grain, resulting in the formation of defects (voids) of the order of the grain size, which connect with adjacent defects (voids), to form micro-cracks. The increase in the number density of grain size defects (voids) is used as an index of actual creep damage [11].

The mechanism of Type IV damage from a continuum-mechanics point of view [12] is considered as follows: creep deformation of a FGHAZ with lower creep strength than the adjacent material is subject to tri-axial constraint by the neighboring base metal and weld metal; and this can promote a high nucleation rate of creep voids subsurface within the FGHAZ, where the tri-axiality is greatest. Regarding CGHAZ (Coarse grained heat affected zone) we would like to add a short comment. In

the creep damage evaluation for 2.25Cr-1Mo steel welds, both FGHAZ (Type IV failure) and CGHAZ (Type III failure) were considered, just as discussed in the related paper [13]. In the case of mod.9Cr-1Mo steel welds, on the other hand, creep voids are mainly observed in FGHAZ, and not in CGHAZ. In Fig.1, we cannot clearly define CGHAZ, but weld-metal-side narrow zone in HAZ is considered as CGHAZ. We assume that the width of CGHAZ is small and creep strength is almost the same as weld metal resulting in higher creep strength than FGHAZ. Tri-axial constraint caused by neighboring materials with higher creep strength, is high in FGHAZ, and low is in CGHAZ.

For simulating the failure process from microscopic damage of the FGHAZ to final fracture of a welded joint, a method using damage mechanics seems to be appropriate, and many works have been reported [14-17]. However, the correspondence between the damage variable and the creep void density, i.e., the physical meaning of the damage variable, has not been sufficiently examined. Fukahori et al. [18, 19] carried out damage simulations using a random-fracture-resistance model of grain boundaries to predict the creep void density distribution of large uniaxial welded joints, and predicted final rupture life using a damage mechanics concept. By comparing the observed creep void density and simulation results, they identified a critical value of the creep void density corresponding to micro-crack initiation.

Honda et al. [20] developed a damage simulation method combining continuum damage mechanics and a void nucleation model (void mechanics model) proposed by Gonzalez and Cocks [21] in which a grain facet of polycrystalline material subject to multiaxial stress is regarded as a void. Honda et al. [20] defined a critical value of creep void density corresponding to micro-crack initiation, and clarified the physical meaning of the damage parameters. This method was applied to notched round bar creep tests of simulated FGHAZ of a modified 9Cr-1Mo steel with uniform hardness, to predict the damage distribution (creep void density distribution) and the rupture time.

In this paper, a creep damage analysis scheme [20] is applied to welded joints with non-uniform weld materials, the HAZ and base metal, such as those found in large uniaxial cross-weld specimens. The influence of hardness distribution in the FGHAZ is examined in the form of the distribution of creep strength in the FGHAZ. Both the predicted creep void density distribution and failure process, consisting of crack initiation, propagation and final rupture are compared with experimental results at 650°C.

2. Creep Damage Analysis Scheme

2.1 Void mechanics and damage models for FGHAZ

Since void nucleation and damage models in the FGHAZ were reported in a previous paper [20], only an outline is given here. A creep constitutive law of the FGHAZ was formulated based on the

model of Perrin-Hayhurst [22] as shown in eq. (1), which considers both mechanical damage due to creep voids and metallurgical damage by strain softening.

$$\dot{\epsilon}_{ij}^c = \frac{3}{2} A \sinh \left[\frac{B \sigma_{eq}}{(1-G)(1-D)} \right] \frac{\sigma_{ij}^D}{\sigma_{eq}} \quad (1)$$

where σ_{ij}^D , σ_{eq} , G , D , A and B are respectively deviatoric stress, von Mises equivalent stress, damage parameter due to strain softening, damage parameter associated with creep voids and two material constants. In this equation, primary creep is neglected, but both secondary and tertiary creep due to damage development and strain softening are considered. The evolution equation for damage G is expressed as eq. (2), where the first term is due to strain softening and depends on the von Mises equivalent creep strain rate $\dot{\epsilon}_{eq}^c$ and yield stress σ_y ; the second term is the time dependent thermal softening; and α , κ and Kc are material constants.

$$\dot{G} = \alpha \left(\frac{\sigma_{eq}}{\sigma_y} \right)^\kappa \dot{\epsilon}_{eq}^c (1-G)^2 + \frac{Kc}{3} (1-G)^4 \quad (2)$$

The damage parameter D due to creep voids is defined by eq. (3) in relation to the creep void area density N (1/mm²).

$$D = \frac{N}{40000} \quad (3)$$

The denominator in eq. (3) is the total number of grains in 1 mm² for an average grain size of 5µm. This number 40000 is derived from the reference [19], in which foursquare shape with an averaged grain size of 5µm is assumed.

The void nucleation model in eq. (4) was proposed by Gonzalez and Cocks [21] as a model applicable to the FGHZ of P91 under a multiaxial state of stress. The base line is the continuous cavity nucleation model for a grain-boundary facet given by Dyson [23], and is considered to have a correspondence with experimental observations by Masuyama et al. [10] as discussed in the introduction; defects (voids) form through the nucleation, growth and coalescence of much smaller cavities around the periphery of a grain. Gonzalez and Cocks [21] assumed that the rate of formation of these grain-sized defects (voids) is determined by the average rate of nucleation of small cavities around the grain perimeter. Gonzalez and Cocks [21] considered the randomness of grain-boundary-facet orientations in a polycrystalline material and provided a damage growth criterion in terms of the creep strain rate and tri-axiality factor X in eq. (5), where σ_m is the hydrostatic stress, defined by the sum of the three principal stresses divided by three.

$$\dot{N} = a \dot{\epsilon}_{eq}^c \left(\frac{4}{9} + \frac{20}{9} X^2 \right) \quad (4)$$

$$X = \frac{3\sigma_m}{2\sigma_{eq}} \quad (5)$$

When comparing the uniaxial tension ($X=0.5$) and equi-biaxial tension ($X=1.0$), for example, the term

$\left(\frac{4}{9} + \frac{20}{9}X^2\right)$ takes a value of “1.0” and “2.67”, respectively. This tendency corresponds with the experimental study of Fujimoto & Sakane [24] using cruciform plate specimens of 2.25Cr-1Mo steel; creep void density under equi-biaxial stress is 2~3 times larger than that under uniaxial stress, when the von Mises stress is the same.

The reduction of Young's modulus by coalescence of voids leading to micro-cracks is considered as shown in eq. (6) following Lemaitre's method [25].

$$E = E_0 \left(1 - \frac{D}{D_{cr}}\right) \quad (6)$$

where E and E_0 are Young's modulus of damaged and non-damaged material, respectively; and D_{cr} is the critical damage corresponding to the initiation of a micro-crack resulting from the coalescence of voids. Based on the comparison of microscopic observations and simulation results by the random-fracture-resistance model of grain boundaries, $N=4000/\text{mm}^2$ is adopted as a critical value for the formation of micro-cracks. The critical damage D_{cr} is then determined as “0.1” from eq. (3). Critical number density of creep void $4000/\text{mm}^2$ was determined based on the previous works by the authors. In the reference [19], we carried out a simulation based on random-fracture-resistance model of grain boundaries to predict time-history of creep void density distribution in mod.9Cr-1Mo steel welds. We compared the obtained results with observed results [11] for through-thickness distribution of voids and cracks, in which FGHAZ in the other side of ruptured FGHAZ was observed. In some area in the thickness, micro cracks are observed, and the simulated results of creep void density at this area was about $4000/\text{mm}^2$. Since creep voids coalesce to each other in the actual situation, counting method of number density of voids is important. In our approach in both simulation and observation, individual void is counted. In the case of coalesced voids composed of four voids, for example, number of voids is counted as four, not one. This method generally gives a larger number when compared with the case counting the coalesced voids as one.

2.2 Identification of creep properties of FGHAZ

Since the critical damage D_{cr} is as small as “0.1”, the role of strain softening in eq. (1) is important in expressing the tertiary stage of creep and rupture time of the FGHAZ. Stress dependence of the creep strain rate and rupture time is a key aspect of predicting the rupture time of welded joints. [Figure 1](#) provides an example of Vicker's hardness (H_v) distribution in weld metal, the HAZ and base metal. Vicker's hardness based on applied loads of 98N is at its highest H_v282 adjacent to the weld interfaces, then gradually decreases in the HAZ and is at its lowest value of H_v191 close to the boundary between the HAZ and the base metal. The width of the FGHAZ, a part of the HAZ, is approximately 2mm, and lies at the boundary with the base metal. Creep deformation and rupture data of the FGHAZ at 650°C were obtained using smooth round bar specimens of the FGHAZ

material after heat treatment simulating a multi-pass weld that reproduces a grain structure similar to the FGHAZ with a hardness Hv191. Figure 2 (a) shows the minimum creep rate of the FGHAZ together with that of the base metal [24]. Minimum creep rates of the FGHAZ are almost one hundred times faster than those of base metal at the same stress. Figure 2 (b) shows the rupture time of the FGHAZ together with that of base metal [26] and the welded joint [27]. Rupture times of the FGHAZ are almost one tenth of those of the welded joint. The experimental data of the FGHAZ in Fig.2(a) and Fig.2(b) are summarized in Table 1; stress level is from 40 to 80 MPa; and new data [28] below 60 MPa are added to those presented in the previous paper [20]. Since creep voids were not found in the FGHAZ creep tests, only the strain softening term in eq. (1) was considered in determining material constants for the FGHAZ. Just as shown in eq. (4), void nucleation rate is influenced by tri-axiality of stress and creep strain rate. Although FGHAZ in welded joint has high tri-axiality of stress resulting in void nucleation just as described in the observation of Masuyama et al. [10], round bar specimen made of uniform FGHAZ has low tri-axiality resulting in ductile failure with negligible creep void nucleation.

Material constants for strain softening were recalculated to cover wider range of stress than that in our previous paper [20]; consideration of the balance in expressing both minimum creep rates and rupture times was a key element of this reevaluation. Table 2 shows material constants for softening used in this paper. Parameters A and B in the table are responsible for expressing the minimum creep rates; and parameters α , κ and K_c play a key role in describing the rupture time. Simulation results using these constants are also depicted in Fig.2 (a) and (b). The simulation results show that the data set in Table 2 provides a better description of the low stress behaviour compared with our previous paper [20]. Figure 3(a) and (b) respectively provide examples of the time history of creep strain rate and creep strain, from both experiment and simulation. Regarding the creep strain rate in Fig.3(a), the simulation results neglect primary creep and this gives rise to some differences with the experimental data, but they provide a good description of tertiary creep behavior. Creep curves in Fig.3(b) reflect the tendency shown in Fig.3(a) and in the last stage of creep life the influence of neglecting primary creep is small. Although verification of simulation results in Fig.2 (b) is expected by comparing with tests below 40MPa, the simulation in this paper can cover the stress level in the experiment of welded joints in Fig.4 with the nominal stress of 66MPa.

Material constants for creep damage (voids) are the same as in the previous paper, as shown in Table 2. Roles of material constants in Table 2 are briefly summarized; A and B are constants describing creep strain rate in eq.(1); α and κ are constants governing the metallurgical damage by strain softening rate in the first term in eq.(2); K_c is a constant governing the metallurgical damage by the time-dependent thermal softening; a is a constant governing the nucleation rate of voids in eq.(4); σ_y is a yield stress of FGHAZ governing the metallurgical damage by strain softening rate in the first term in eq.(2). Determination process of material constants will be shown in the

followings. Since the creep voids were not found in the smooth round bar specimens of the FGHAZ material due to the low value of tri-axiality factor in the specimen, creep strain rates in Figs.3(a) and (b) were compared with eq.(1) with $D=0$. In this process compatibility with minimum creep rate in Fig.2(a) is considered. Contribution of K_c i.e. time-dependent thermal softening is also considered, but the contribution of this term is small in the conditions in our paper. Material constant a was determined to express the creep void density distributions in round bar notched specimens of uniform FGHAZ material with sharp and blunt notch [20]. Profile of creep void density distribution is governed by tri-axiality factor and creep strain rate as shown in eq.(4). Constant a was determined to express the peak value in sharp notch specimen, but could express the distribution in both sharp and blunt notch specimens [20]. Compared with the material constants in the previous work [20], parameters a and σ_y are not changed; parameters A , B , α , κ and K_c are reexamined based on the additional data at low stress level in Table 1. The keys of reexamination are to express the creep strain behavior in Figs.3(a) and (b), and to express the creep rupture life in Fig.2(b).

Table 1 Results of uniaxial creep tests of FGHAZ material

Temperature (°C)	Stress (MPa)	Rupture life time (h)	Minimum creep strain rate (mm/mm/h)	Reference
650	80	74.0	1.21.E-03	Honda [20]
650	70	172.5	6.11.E-04	Arisue [28]
650	60	448.0	1.63.E-04	Honda [20]
650	55	763.2	1.49.E-04	Arisue [28]
650	45	2181.0	4.87.E-05	Arisue [28]
650	40	5730.7	1.56.E-05	Arisue [28]

Table 2 Material parameters used in the analysis

A (1/h)	B (-)	α (h)	κ (-)	K_c (-)	a (1/mm ² /h)	σ_y (MPa)
4.0×10^{-7}	0.105	1.0	2.0	2.0×10^{-4}	0.0375	200.0

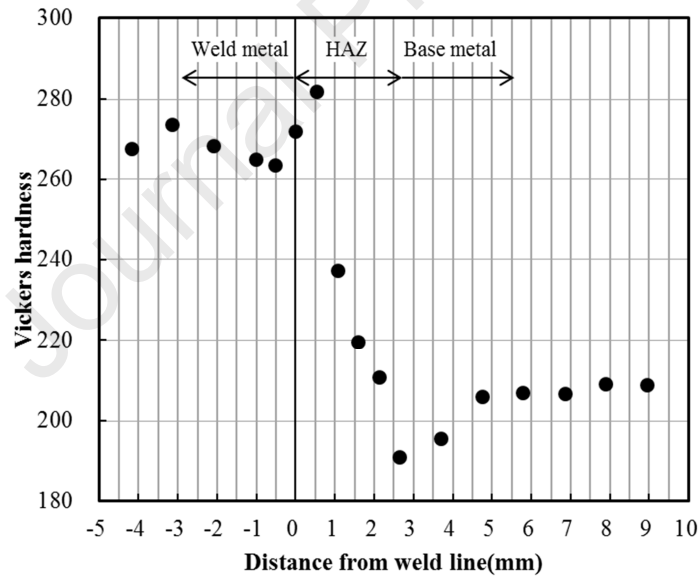


Figure 1 Vickers hardness distribution in a welded joint

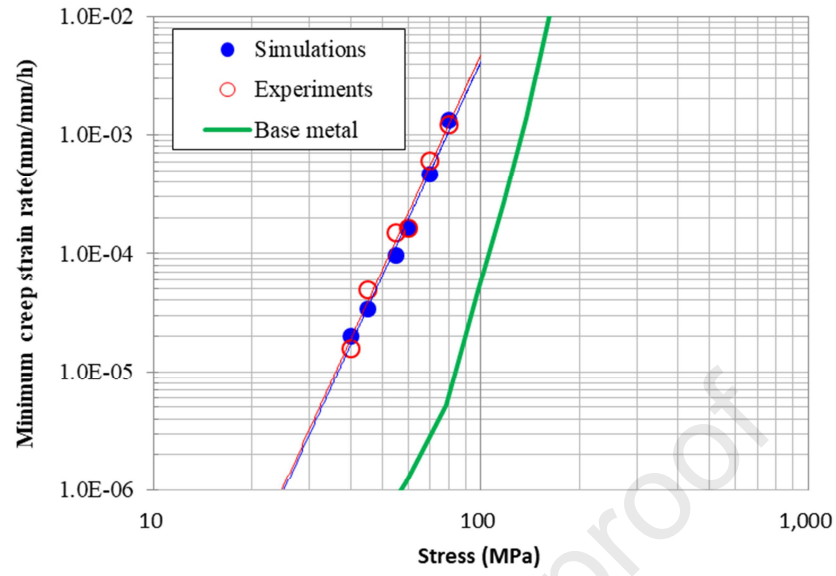


Figure 2 (a) Minimum creep rate of FGHAZ material at 650°C

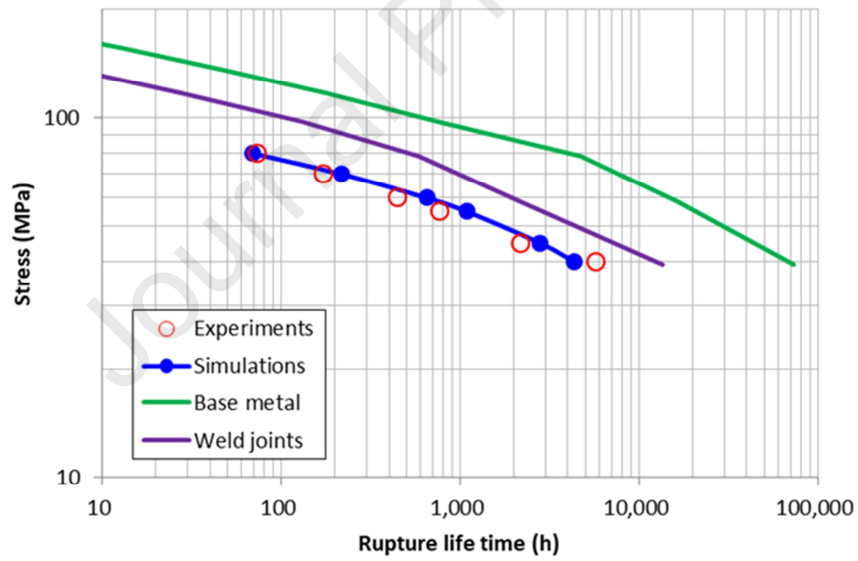


Figure 2 (b) Creep rupture life of FGHAZ material at 650°C

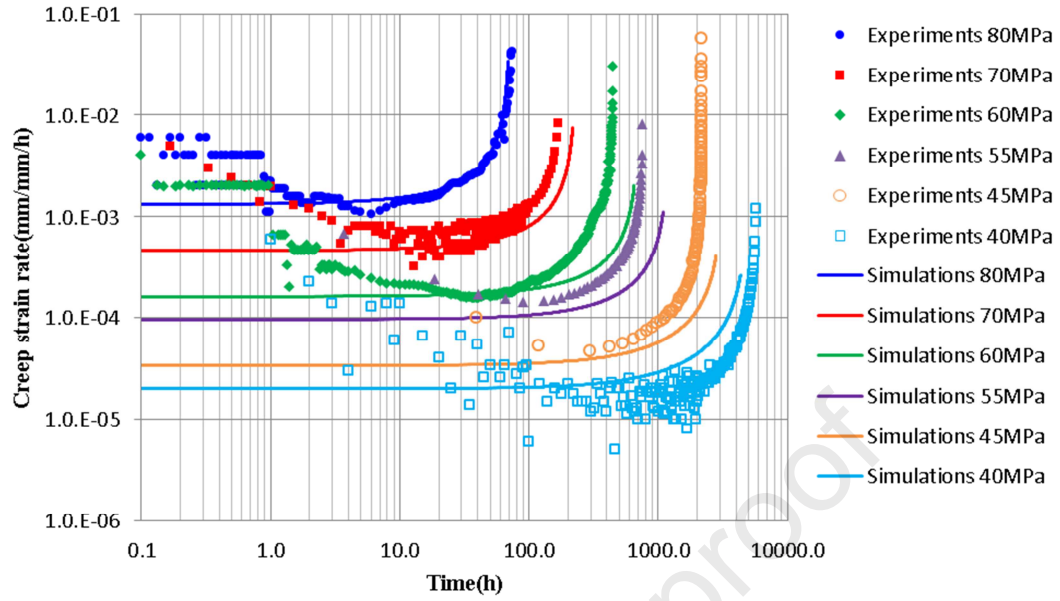


Figure 3(a) Time history of creep strain rate of FGHAZ material at 650°C

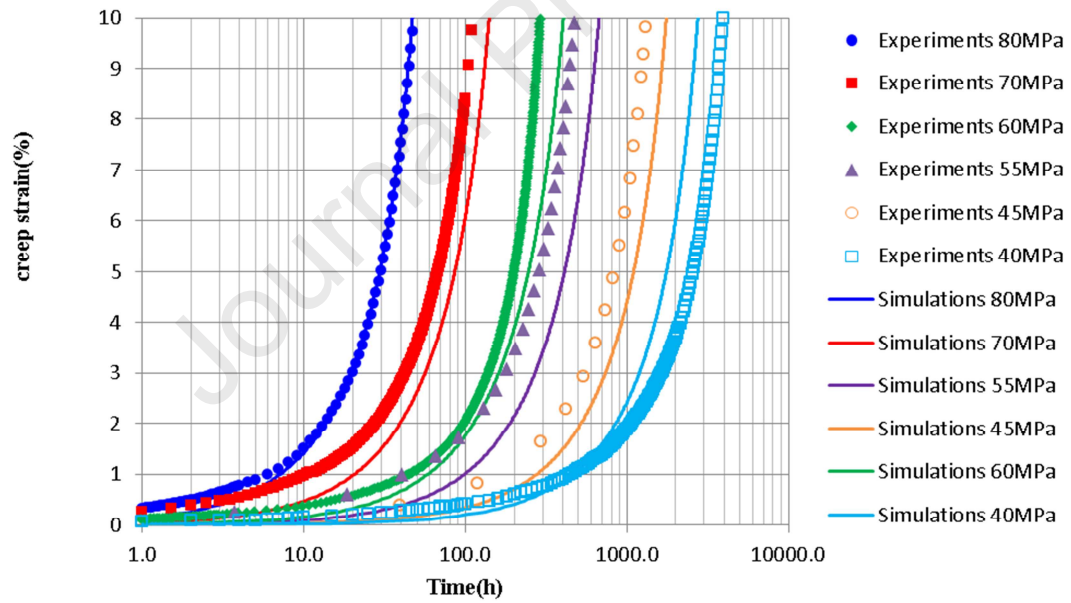


Figure 3(b) Creep curves for FGHAZ material at 650°C

2.3 Creep equations for weld metal and base metal

Just as discussed in Introduction, the width of CGHAZ is small and creep strength is almost the same as weld metal. We assume that creep properties of CGHAZ are the same as those of weld metal. Since the creep strain in both weld metal and base metal is smaller than for the FGHAZ, which has a lower hardness, a conventional primary and secondary creep equation is adopted for weld metal and base metal as described in eq. (7).

$$\varepsilon_c = C_1\{1 - \exp(-r_1 t)\} + C_2\{1 - \exp(-r_2 t)\} + \dot{\varepsilon}_m t \quad (7)$$

Material parameters in eq. (7) are listed in [Table 3](#) for plate material for large cross weld specimen and in [Table 4](#) for pipe material for circumferentially welded pipe, respectively. Rupture time equations for plate and pipe are taken from the references [26] and [27], respectively. Minimum creep rates are determined from rupture equations [26, 27] and Monkman-Grant relation [29]. Equations for primary creep are taken from the reference [29]. Since rupture equations employ 2nd-order polynomials having maximum rupture time at certain stress level, they are only applicable to the stress level above that point, 8MPa for plate and 3MPa for pipe. Below these stresses, rupture time is set as inversely proportional to the ratio of applied stress to stresses at these points. Rupture equations in Table 3 and Table 4 show average trend of the available data for base metal. Creep strain and void nucleation characteristics in Table 2 are average trend for one FGHAZ material. Possible deviation of these properties can have some influence on the simulation results such as creep void density and rupture life. This point is left for future study.

Table 3 Properties for determining creep strain for plate

t_r	$Min(t_{r1}, t_{r2})$
	$\log(t_{r1}) = (21394.7 + 17215.4(\log\sigma) - 6026.6(\log\sigma)^2)/T - 31.55$
	$\log(t_{r2}) = (22479.5 + 3733.3(\log\sigma) - 2117.3(\log\sigma)^2)/T - 20.11$
$\dot{\varepsilon}_m$	$0.1380 t_r^{-1.204}$
C_1	$2.13822 \dot{\varepsilon}_c^{0.59235} / r_1$
C_2	$0.927675 \dot{\varepsilon}_c^{0.8165} / r_2$
r_1	$317.0902 t_r^{-0.56858}$
r_2	$14.3245 t_r^{-0.82278}$
Note: t_r [h], σ [MPa], T [K], $\dot{\varepsilon}_m$ [mm/mm/h]	

Table 4 Properties for determining creep strain for pipe.

t_r	$Min(t_{r1}, t_{r2})$
-------	-----------------------

$$\begin{aligned}
\log(t_{r1}) &= (27140.7 + 12714.9(\log\sigma) - 5079.8(\log\sigma)^2)/T - 32.30 \\
\log(t_{r2}) &= (35063.7 + 2366.9(\log\sigma) - 2423.4(\log\sigma)^2)/T - 29.88 \\
\dot{\epsilon}_m &= 0.1380 t_r^{-1.204} \\
C_1 &= 2.13822 \dot{\epsilon}_c^{0.59235} / r_1 \\
C_2 &= 0.927675 \dot{\epsilon}_c^{0.8165} / r_2 \\
r_1 &= 317.0902 t_r^{-0.56858} \\
r_2 &= 14.3245 t_r^{-0.82278}
\end{aligned}$$

Note: t_r [h], σ [MPa], T [K], $\dot{\epsilon}_m$ [mm/mm/h]

3. Outline of Experimental Results for Welded Joints.

3.1 Uniaxial creep tests for large cross weld specimens

Komai et al. [11] conducted creep tests at 650°C under a stress of 66 MPa on modified 9Cr-1Mo steel specimens (extracted from a plate) of rectangular cross section 42 mm wide by 32 mm thick, with X- and U-grooves. The rupture time and the cross section after rupture of each specimen are shown in Fig. 4. The rupture time was 2049 hours for the X-groove and 2775 hours for the U-groove specimen respectively. Voids were detected in the FGHAZ and cracks were found along the FGHAZ of both specimens.

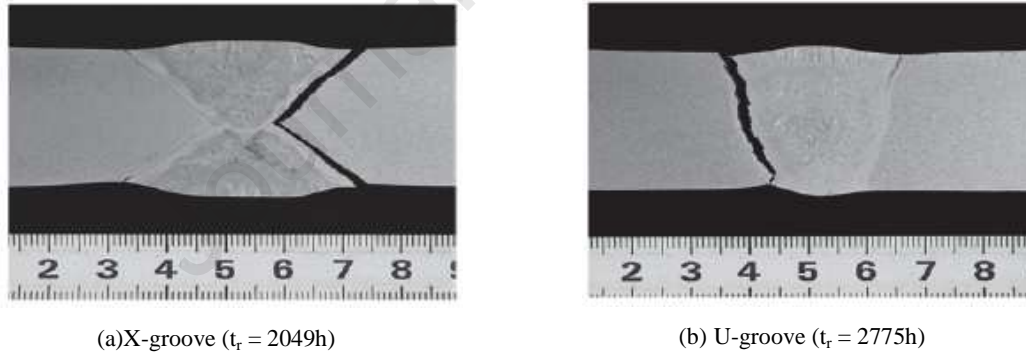


Figure 4 Macrostructures after failure of large uniaxial cross weld specimens [11]

3.2 Internal pressure and bending creep test of circumferentially welded pipes

As shown in Fig. 5, Nishinoiri et al. [30] conducted a creep test on a modified 9Cr-1Mo seamless steel pipe with an outer diameter of 686 mm and a thickness of 30 mm at 650°C (630°C during 3500~4224 hours), in which both an internal pressure of 3.9 MPa and a four-point bending load with a nominal elastic bending stress of 36.8 MPa at the outer surface at the center of the specimen (C-C section in Fig. 5) were applied. There are two circumferential joints, joint-A and B at the center of the specimen. At 3500 hours from the start of the test, crack-like damage at the mid-wall of the

thickness was detected by phased array ultrasonic testing (PAUT); and the crack-like damage was considered to propagate towards the inner surface of the pipe. The test was interrupted after 6930 hours, when a surface crack at the outer surface was found along the circumferential joint-A. The test concluded at this time, because the creep damage in the thickness was confirmed from the result of PAUT. Figure 6 [30] shows the results of PAUT in the circumferential and thickness directions of joint A at both 3500 and 6930 hours; at 3500 hours nonconsecutive damage due to creep voids was detected; at 6930 hours similar damage was found near the inner surface in the area $\pm 45^\circ$ to the circumferential direction and 15mm in the thickness direction. Figure 7 [30] shows a cross-sectional micrograph of joint-A where damage was found by PAUT. Cracks were confirmed in the left FGHAZ region. Though the cracks almost penetrated to the outer surface, the cracks in the left FGHAZ did not penetrate to the outer surface. This implies that surface cracks at the outer surface were considered to be independent of cracks in the thickness.

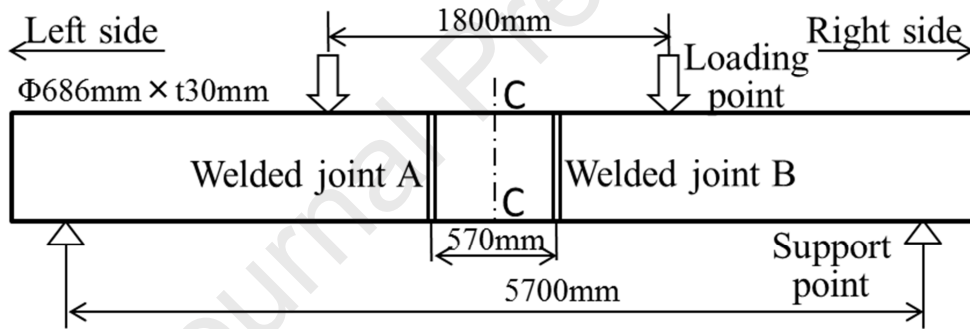


Figure 5 Testing set up of circumferentially welded pipe under inner pressure/axial bending

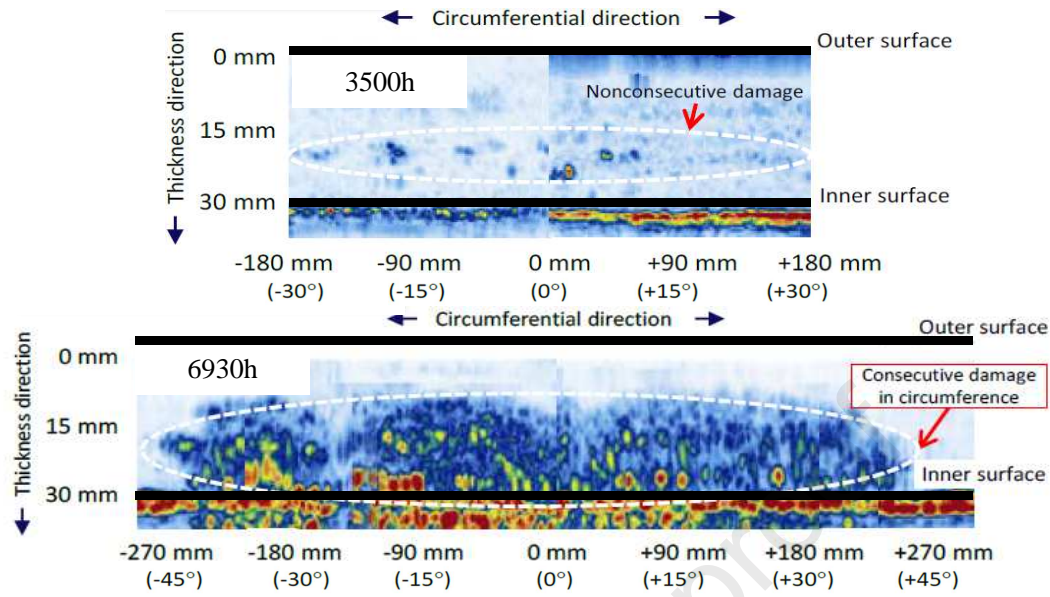


Figure 6 PAUT results of joint A at 3500h and 6930h [30]

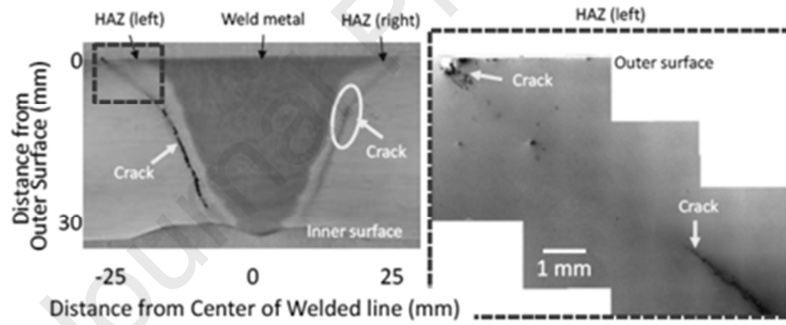


Figure 7 Cross sections after failure of circumferentially welded pipe (joint A, $t_r = 6930h$) [30]

4. Damage Analysis of Creep Tests for Large Uniaxial Cross Weld Specimens

4.1 Analysis method

The X-groove and U-groove specimens in Fig.4 are analyzed using the commercial FEM code ABAQUS (ver. 6.12-2) and the generalized plane strain element (CPEG4R and CPEG3). Figure 8 shows FEM models for large uniaxial cross weld specimens, which are determined from a photograph of one side of the test specimen.

When considering the distribution of hardness in the HAZ as shown in Fig.1, two different approaches were adopted in modeling the FGHAZ with a width of 2mm; one is a simple model based on the lowest hardness Hv191 (uniform model: Model-1) and the other considers a hardness gradient (gradient model: Model-2).

The method of setting the material properties of Model-1 and Model-2 is now described in detail. Figure 1, as discussed in section 2.2, shows the hardness distribution in a welded joint in an elbow fabricated from a base material of the same lot as the test specimens. The hardness changes from the weld metal to the base metal. The HAZ, from the melting boundary to the base metal side in the figure, consists of a narrow coarse grain zone, a wide fine grain zone (FGHAZ), and a narrow inter-critical HAZ with the lowest hardness. Since the width of the FGHAZ is the largest, a three-material model consisting of weld metal, the FGHAZ and the base material is adopted in the following analysis. Four FEM elements were used for the FGHAZ region with a width of approximately 2 mm. In Model-1, uniform creep properties for a material with a hardness Hv191 were assigned across the four elements of the FGHAZ. A method to consider the hardness distribution in the FGHAZ in Model-2 is based on the first term of equation (2); the yield stress of the material is used as an index of the resistance of the material to strain softening; and proportionality between material hardness and yield stress is assumed to predict a creep strain rate depending on the hardness. Hardness is determined based on indentation size caused by plastic deformation. Proportionality of hardness and tensile strength is well known. Proportionality of hardness and yield stress is also discussed for various materials [31], in which data for low alloy steel are shown. The method to predict yield stress of FGHAZ is as follows; Hardness of uniform FGHAZ material was Hv193 [20], and yield stress at 650°C is assumed to be 200MPa as shown in Table 2, same value as base material (from Sumitomo Metal Creep Data Sheet (1972)); Yield stress with different hardness was predicted by multiplying 200MPa with the ratio of hardness.

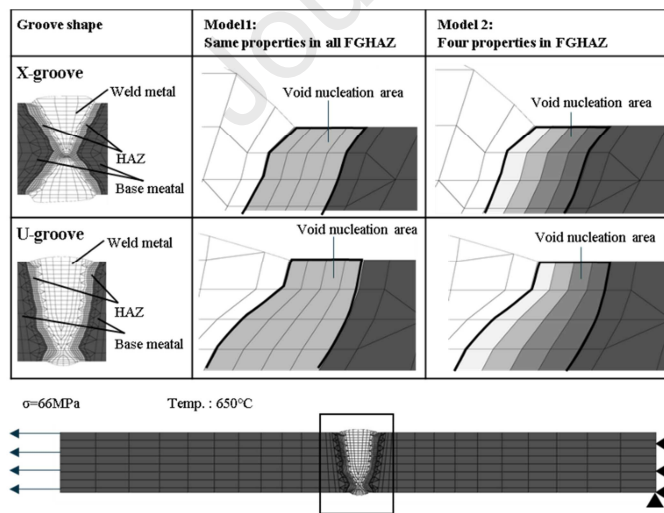


Figure 8 FEM model of large uniaxial cross weld specimen

4.2 Analysis of results.

The creep void density distribution for X- and U-groove specimens at the rupture time are shown in

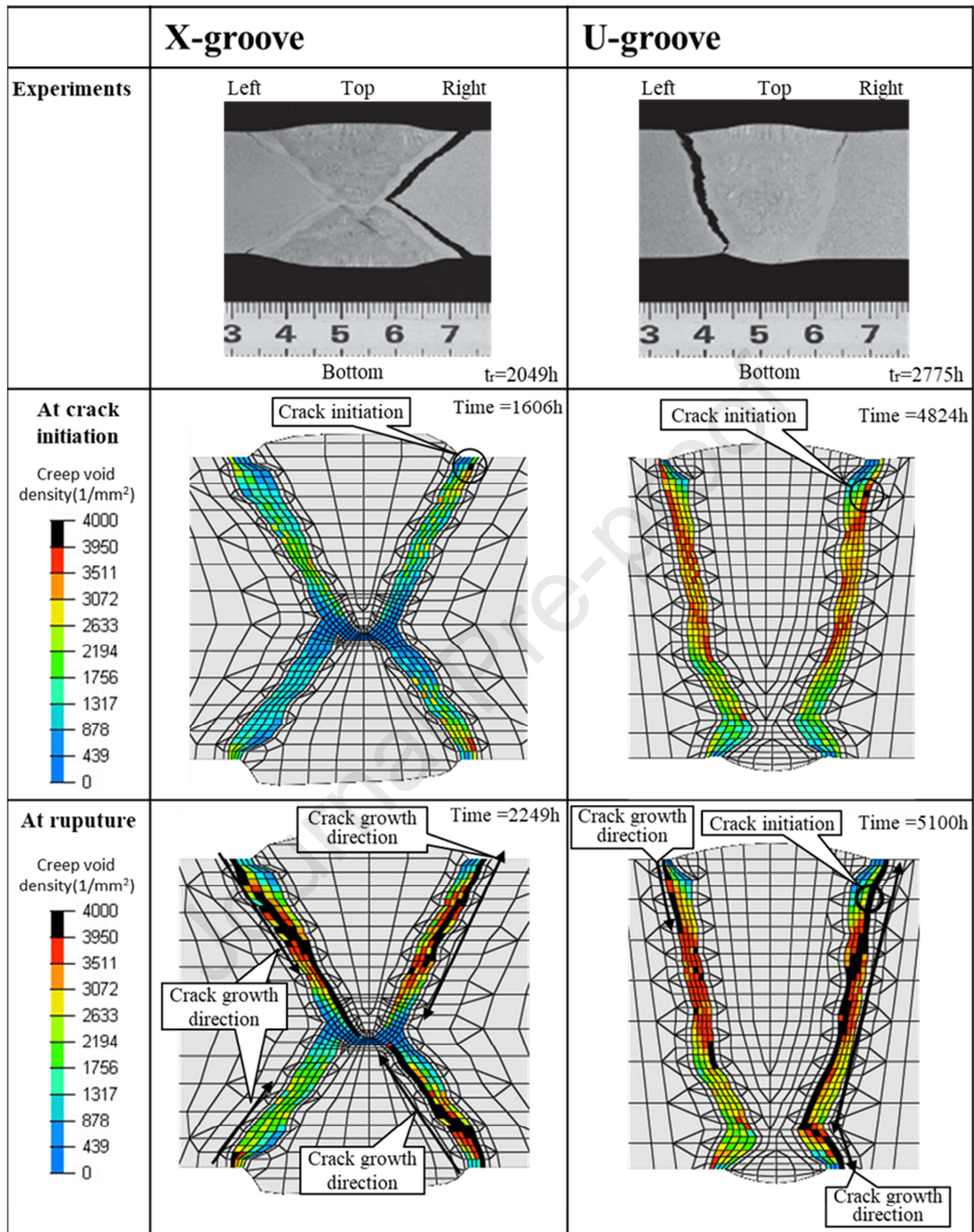
Fig. 9 for Model-1. The rupture time from the analysis is determined as the time when an abrupt increase in creep deformation caused by penetration of cracks through the FGHAZ thickness is observed. The black zone in Fig.9 indicates the cracked area, defined as having a creep void density over $3950/\text{mm}^2$, i.e. initiation of micro-cracking. Cracks initiated from the subsurface and propagated through the FGHAZ thickness. Arrows in the figure designate the crack propagation path in the FGHAZ. The difference in the results from Model-1 and 2 are negligible, including the crack initiation location and crack path. Analysis results for crack initiation and crack path almost correspond with the experimental results shown in the figure. The creep void density $3950/\text{mm}^2$ is used as a numerical measure of critical void density $4000/\text{mm}^2$ as shown sec. 2.1. Since the critical void density depends on microstructure and chemical contents, further study is expected on the applicability of this value to general Gr91 steel welds.

Figure 10 expresses the rupture time from analysis and experiment; the ratio of predicted and experimental rupture time was 1.1 for X-groove and 1.8 for U-groove, i.e. within a factor of 2. There is little difference in the analysis results for Model-1 and 2; rupture time for the X-groove sample predicted by the analysis is 2250 hours (Model-1) and 2260 (Model-2); and that predicted for the U-groove is 5100 hours (Model-1) and 5100 (Model-2). The reason for the small difference between Model-1 and 2 is that the damage progress in the FGHAZ adjacent to the base metal, where the hardness has its minimum value, is dominant in determining rupture lives of welded joints; and therefore the damage progress in the FGHAZ is almost the same in Model-1 and 2. The ratio of crack initiation and rupture time from analysis as shown in Fig.10 is 0.95 and 0.71 respectively for U and X-groove samples. The case of X-groove, with larger stress gradient, showed a longer time for crack propagation compared with the U-groove sample. This is the same tendency as shown in our previous paper [19] using the random-fracture-resistance model of grain boundaries on both a large uniaxial cross weld specimen with U-groove and an actual-size elbow with the same U-groove and thickness subject to internal pressure; crack initiation life (defined by a damaged area of 2mm in the thickness) for the former case was 0.94, and 0.72 for the latter case which has a larger stress gradient in the thickness.

Contour diagrams of three parameters in eq. (4), i.e. creep void density, equivalent creep strain and tri-axiality factor, are shown respectively in Fig.11 (a)-(c) in for U-groove at crack initiation ($t/t_r=0.5$, t_r : rupture time from analysis) and just before rupture ($t/t_r=0.8$). Setting of material properties is based on elements. Fig.11 shows simulated results at the center of element, and horizontal axis is taken from the center of element at the weld metal side. Contour scales in the figures are common at the above two times. Examples of the distribution of the above three parameters through the width of the FGHAZ are also shown in the figures. With respect to the distribution through the width of the FGHAZ, an FEM element neighboring the base metal shows a higher creep void density, reflecting the distribution of equivalent creep strain and tri-axiality factor within the FGHAZ. When focusing

on the through-thickness distribution along the FGHAZ neighboring base metal, a similarity with the case of a sharp notch shown in our previous paper [20] is found; equivalent creep strain at the upper surface is large; and creep void density is large subsurface as a result of a combination of the equivalent creep strain and tri-axiality factor.

There is discussion in [32] whether the point with the lowest hardness in the FGHAZ in Fig.1 is the point with the maximum creep void density. Microscopic observations [33] suggest that the hardness distribution can change during the creep process and the point with the lowest hardness can move towards the weld metal side. The point with the maximum creep void density is then found to shift a little further towards the weld metal side. In this paper, an initial hardness distribution was used to determine material parameters, and further study can be conducted reflecting the above discussion from metallurgical findings.



○ : Crack initiation location → : Crack growth direction

Figure 9 Creep void density distribution at rupture from damage analysis of a large uniaxial cross weld specimen

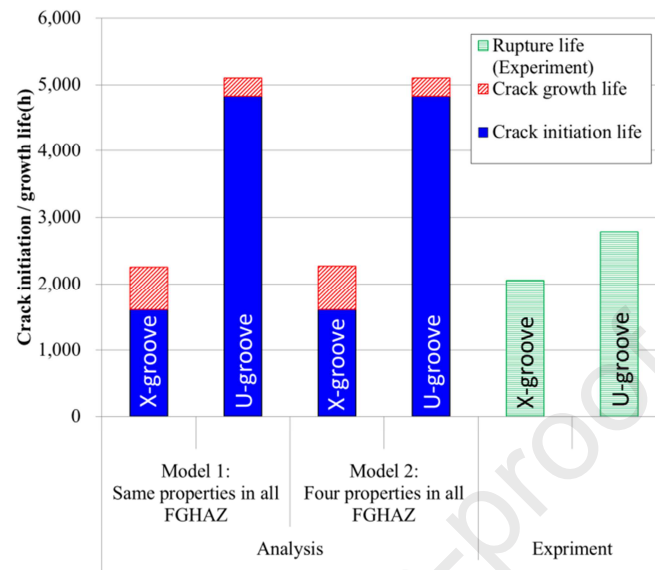


Figure 10 Crack initiation, growth and rupture life in large uniaxial cross weld specimens

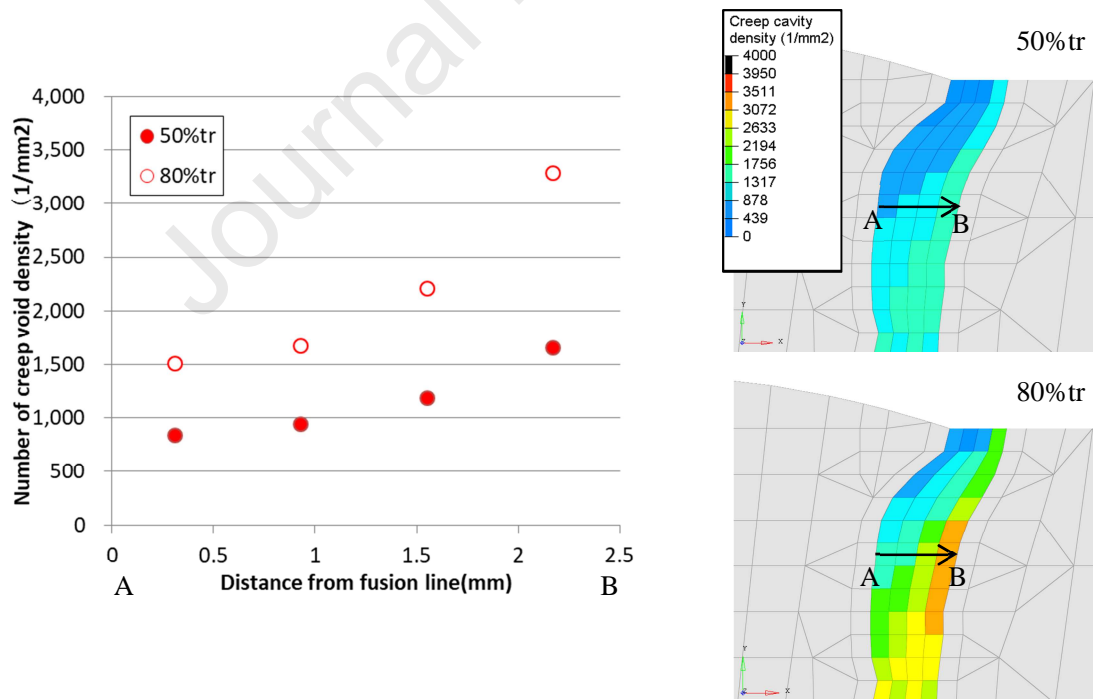


Figure 11 (a) Distribution of creep void density within the FGHAZ

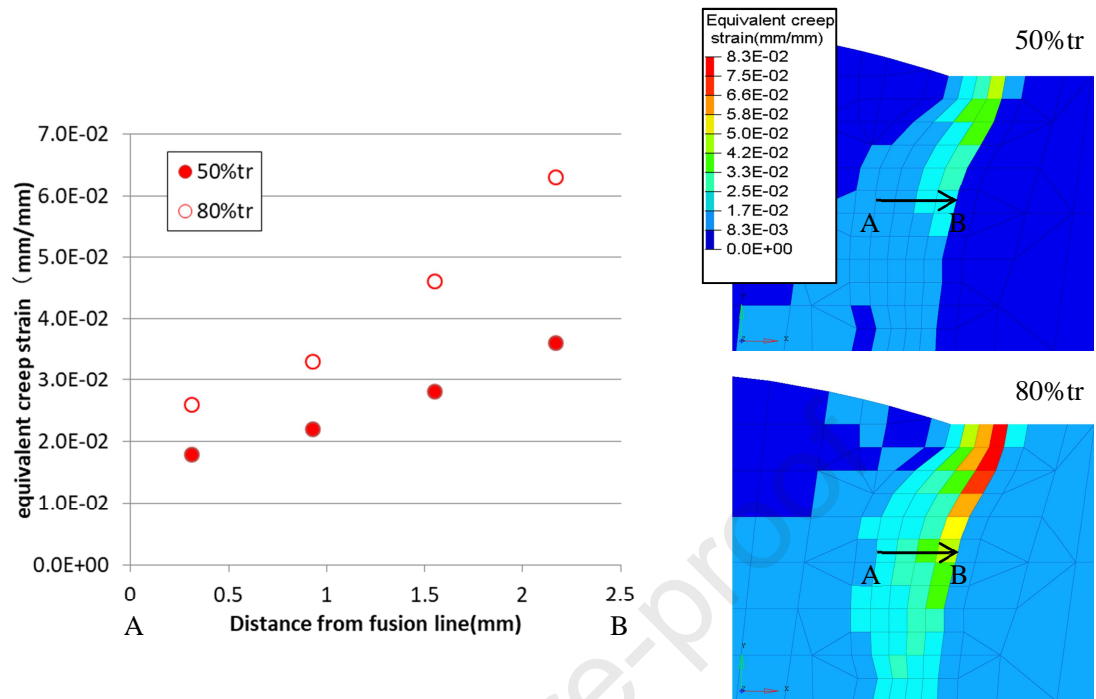


Figure 11 (b) Distribution of equivalent creep strain within the FGHAZ

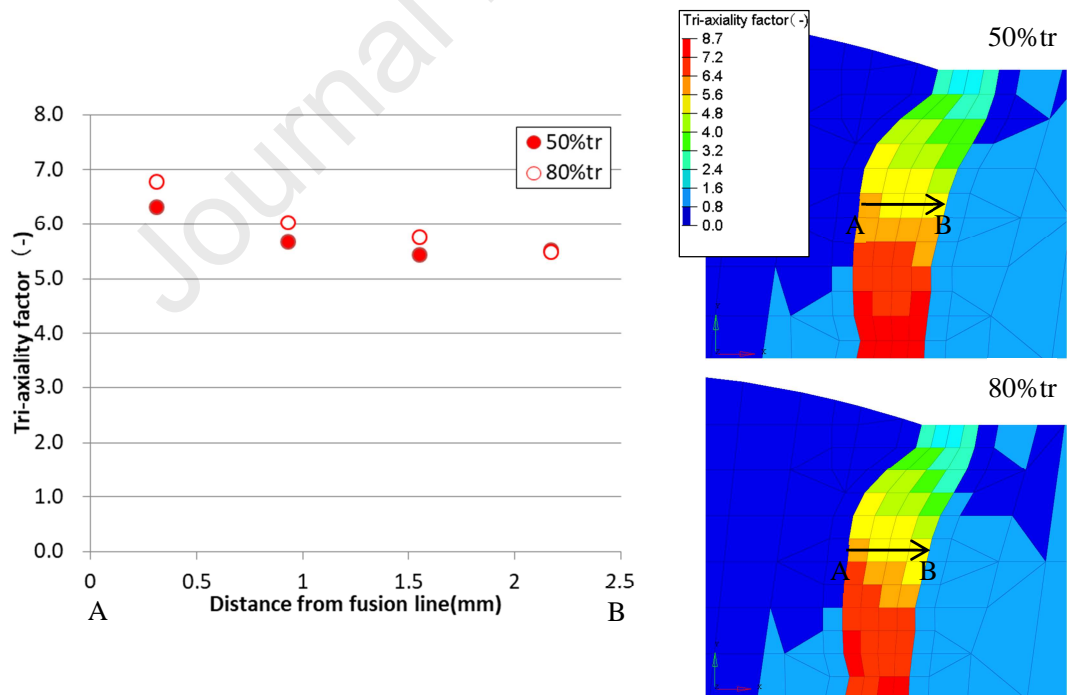


Figure 11 (c) Distribution of tri-axiality factor within the FGHAZ

5. Damage Analysis of Circumferentially Welded Pipe

5.1 Analysis method

The FEM model was a one-fourth-scale model consisting of half of the length and circumference of the pipe considering a symmetrical configuration as shown in Fig.12. A hexahedral solid element C3D8RH and a triangular-prism solid element C3D6H in the commercial code ABAQUS (ver.6.12-2) were employed together with symmetry boundary conditions at the symmetrical surfaces. Creep properties were assigned to the high-temperature parts shown in red and neglected in non-heated parts. Young's modulus and Poisson's ratio were 161GPa and 0.3, respectively. A magnified region of the welded joint is shown in the figure, which was determined from a hardness measurement at a section of the pipe [34]. Just like the case of large cross weld specimens in sec.4.1, three-material model composed of weld metal, FGHAZ and base metal is adopted in this section. Creep properties of weld metal and base metal are depicted in Table 4. Just as discussed in Introduction, the width of CGHAZ is small and creep strength is almost the same as weld metal. We assume that creep properties of CGHAZ are the same as those of weld metal. According to the definition in the reference [34], the HAZ in the model consists of two zones; a "hardened HAZ" with 2mm width (four layers) from the fusion line and a "softened HAZ" outside 2 mm width (four layers). In this paper, the four layers of the softened HAZ with a width of 2mm were regarded as the FGHAZ, and creep properties of hardened HAZ are taken as the same as weld metal. As a first step of evaluating a circumferentially welded pipe, the Model-I with uniform creep characteristics in the FGHAZ was adopted. The creep constitutive law for the FGHAZ is basically the same as that of the plate material in Table 2, but the parameter A is taken as $2.42\text{E-}7$ instead of $4.00\text{E-}7$, reflecting the data in the related paper [35]. In the reference [35] by Honda et al., material constants for plate such as $A=4.00\text{E-}7$ were used for the circumferentially welded pipe. Since pipe material has higher creep strength and lower creep strain rate, the value of A was changed to $2.42\text{E-}7$, remaining other constants unchanged. The creep constitutive law for the weld metal, base metal and hardened HAZ is designated in Eq. (7) with the characteristics of piping material [27] in Table 4.

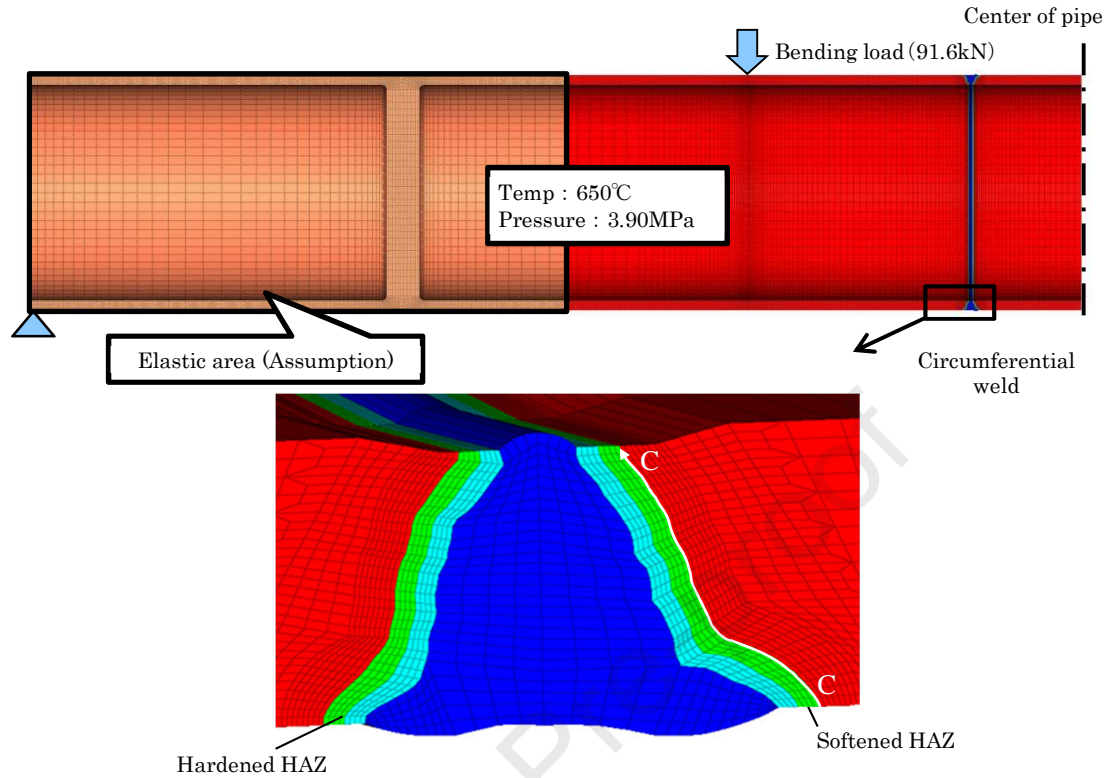


Figure 12 FEM model of circumferentially welded pipe joint

5.2 Analysis results

Figure 13 shows a contour diagram of the creep void density distribution for 1990($0.40t_{pred}$), 3250($0.65t_{pred}$: crack initiation in the thickness), 4470($0.90t_{pred}$: crack growth in the thickness) and 4970($1.00t_{pred}$: penetration to inner surface) hours. Regions with a creep void density exceeding $3950/\text{mm}^2$ are shown in black. Just as shown in sec. 4.2, the creep void density $3950/\text{mm}^2$ is used as a numerical measure of critical void density $4000/\text{mm}^2$ as shown sec. 2.1. Since the critical void density depends on microstructure and chemical contents, further study is expected on the applicability of this value to general Gr91 steel welds.

Crack initiation was found near the central part of the wall thickness; the crack propagated to both the inner and outer side of the pipe; propagation to the inner side was faster than that to the outer side; the crack penetrated to the inner surface; and an independent crack at the outer surface was found at the time of rupture. The damage progress in the thickness direction corresponded well with test results in section 3.2. The crack penetration time to the inner surface was respectively 6930 hours from the test and 4970 hours from analysis. The ratio of penetration time from analysis and experiment was 0.7, i.e. within a factor of 2, and was improved from 0.4 determined by the previous work [35] using the FGHAZ properties of a plate. The crack initiation time, on the other hand, was 3500h in the experiment in which PAUT indications of nonconsecutive creep damage were broadly

detected in the left HAZ of welded joint A [30], and 3000h from analysis; the definition of crack initiation time in the analysis is the time when creep void density in one FEM element reaches $3950/\text{mm}^2$. The ratio of crack initiation and penetration time of 0.65 from analysis compares with 0.53 from experiment. When compared with the large uniaxial cross weld specimens, the time for crack propagation is longer in the case of circumferential welds.

The damage distribution in the circumferential direction along the cc-line in Fig.12 is shown in Fig.14; the angle of the damaged area from analysis was $\pm 58^\circ$, slightly larger than $\pm 45^\circ$ from PAUT at the end of the test; the damage progress behavior in the circumferential direction was almost reproduced by the analysis.

The results shown in Figs.13 and 14 suggest that the damage analysis can be applied to the life prediction of actual components, by identifying the analysis results that give the same damage as the components. In other words, a nondestructive inspection of actual pipe welds is carried out as a first step to determine the current damage after time t ; then we can determine the analytical results which give a similar distribution of damage; the analysis results inform us of the damage ratio t/t_r . We can finally predict the rupture time t_r from the operating time t of the pipe welds.

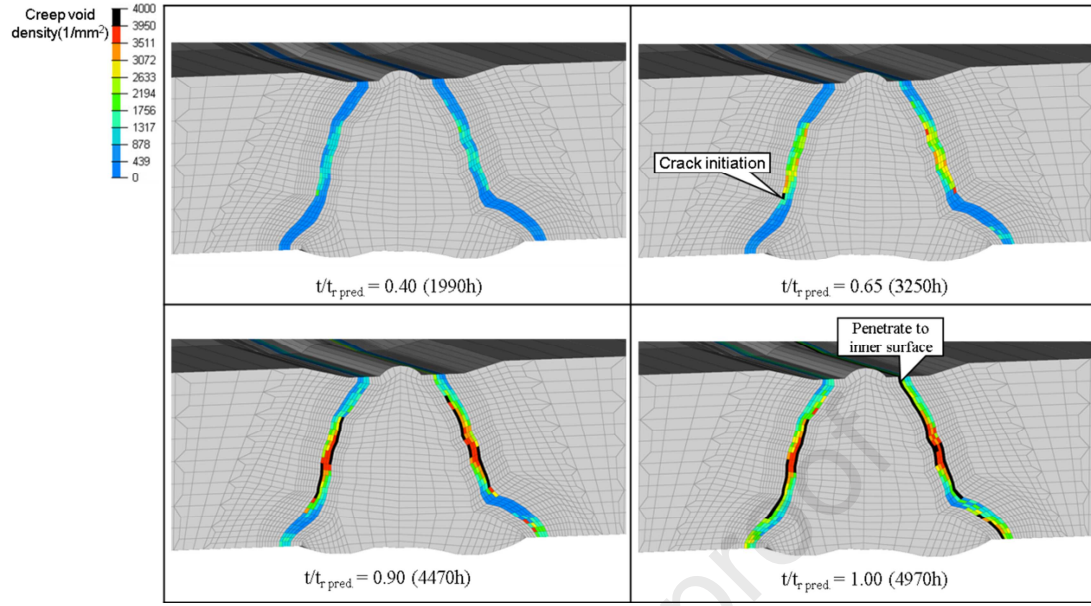


Figure 13 Creep void density distribution on the axial cross-section from damage analysis of circumferentially welded pipe joint

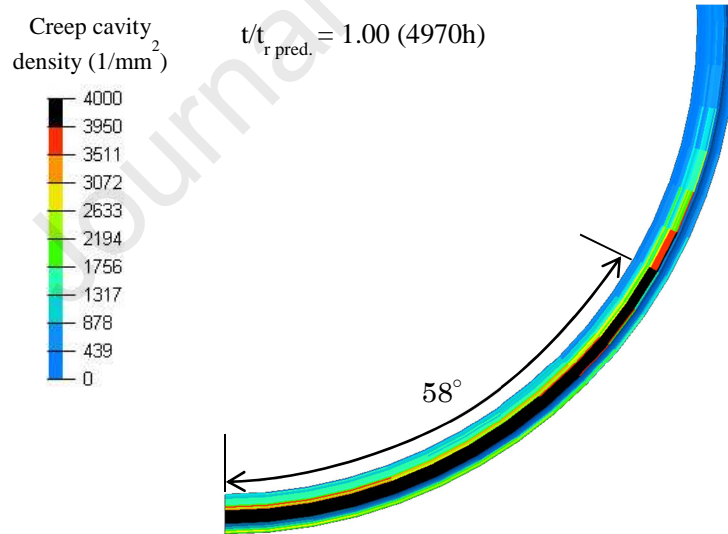


Figure 14 Creep void density distribution on the circumferential cross-section from damage analysis of circumferentially welded pipe joint

6. Concluding Remarks

In order to develop a method to evaluate the remaining life for Type IV damage of modified 9Cr-1Mo steel welds, a damage analysis method combining a void mechanics model and continuum

damage mechanics has been applied to existing experiments at 650°C. The analysis considered creep characteristics of weld metal, the FGHAZ and base metal; especially the stress dependence in the characteristics of the FGHAZ, which has been newly determined. The obtained results are summarized as follows.

(1) In the analysis of uniaxial creep tests for large cross weld specimens, two types of models for the creep characteristics of the FGHAZ have been adopted, i.e. a uniform model (Model-1) and a gradient model (Model-2). Both models gave similar predictions of crack initiation, propagation behavior and rupture life. For the case of an X-groove weld profile, with a larger stress gradient, showed a longer time for crack propagation when compared with a U-groove specimen. Predicted rupture lives of X- and U-groove specimens were within a factor of 2 when compared with experimental results.

(2) In the analysis of the internal pressure/bending creep tests of circumferentially welded pipes, predictions of crack initiation within the thickness and propagation to the inner surface of a pipe showed the same trends as the experimental results. Predicted failure life to crack penetration to the inner surface was within a factor of 2 when compared with experimental results. The ratio of crack initiation and penetration times of 0.65 from analysis corresponded with 0.53 from experiment.

The predicted circumferential length of the damaged area near the inner surface at failure also corresponded with experiment. Since the life consumption ratio at crack initiation and the subsequent progress of damage was almost the same in both analysis and experiment, the possibility of predicting the experimental failure life was demonstrated. First step is searching the analysis results with the same damage as the experiment, and the second step is to predict the experimental failure life from the life consumption ratio obtained by analysis.

References

- [1] F. Abe, and M. Tabuchi, "Microstructure and creep strength of welds in advanced ferritic power plants steels", *Science and Technology of Welding and Joining*, Vol. 9, Issue 1 Issue 1 (2004) 22-30.
<https://doi.org/10.1179/136217104225017107>.
- [2] F. Masuyama, "Creep degradation in welds of mod. 9Cr-1Mo steel", *Int. J. Pressure Vessels and Piping*, Vol.83, Issue 11-12 (2006) 819-825. <https://doi.org/10.1016/j.ijpvp.2006.08.010>.
- [3] J. Hu, T. Fukahori, T. Igari, Y. Chuman, ACF. Cocks, "Modelling of creep rupture of ferritic/austenitic dissimilar weld interfaces under mode I fracture", *Engineering Fracture Mechanics*, Vol.191 (2018) 344-364. <https://doi.org/10.1016/j.engfracmech.2018.01.001>.
- [4] J. Hu, E.El mukashfi, T. Fukahori, T. Igari, Y. Chuman, ACF. Cocks, "Effect of weld angle on the creep rupture life of ferritic/austenitic dissimilar weld interfaces under remote mode I fracture", *Engineering Fracture Mechanics*, Vol.218, 106606 (2019).
<https://doi.org/10.1016/j.engfracmech.2019.106606>.

- [5] M. Tabuchi and Y. Takahashi, "Evaluation of creep strength reduction factors for welded joints of modified 9Cr-1Mo steel (P91)", ASME 2006 Pressure Vessels and Piping/ICPVT-11 Conference Volume 6: Materials and Fabrication, Vancouver, BC, Canada, July 23–27, (2006).
<https://doi.org/10.1115/PVP2006-ICPVT-11-93350>.
- [6] T. Ogata, T. Mitsueda and H. Sakai, "Influence of axial load on internal pressure creep of Mod.9Cr-1Mo circumferential welded pipe", Trans. JSME, Vol.81, No.827 (2015), p.15-00021.
<https://doi.org/10.1299/transjsme.15-00021>.
- [7] T. Himeno, Y. Chuman, T. Tokiyoshi, T. Fukahori, T. Igari, "Creep rupture behavior of mod. 9Cr-1Mo steel pipe subject to internal pressure and axial load", Materials at High Temperatures, Vol.33, Issue 6 (2016) 636-643. <https://doi.org/10.1080/09603409.2016.1226703>.
- [8] K. Arisue, N. Komai, K. Tominaga, M. Fujita, "Microstructures of fine-grained HAZ and long-term creep rupture strength in mod.9Cr-1Mo steel weldments", 4th International Creep Conference ECCC (2017).
- [9] JA.Siefert and JD. Parker, "Evaluation of the creep cavitation behavior in Grade 91 steels", Int. J. Pressure Vessels and Piping, Vol.138 (2016) 31-44.
<https://doi.org/10.1016/j.ijpvp.2016.02.018>.
- [10] F. Masuyama and T. Yamaguchi, "Creep damage initiation mechanism and life of martensitic structures", Proc. of 51st Symposium on High-Temperature Strength of Materials, pp.110-114 (2013).
- [11] N. Komai, T. Tokiyoshi, T. Igari, H. Ohyama, F. Masuyama and K. Kimura, "Experimental observation of creep damage evolution in seam-welded elbows of mod. 9Cr-1Mo steel", Materials at High Temperatures vol.33 Issue 6 (2016) 615-625.
<https://doi.org/10.1080/09603409.2016.1204063>.
- [12] M. Okazaki, ed., "High temperature strength of materials", The Society of Materials Science, Japan, p.448 (2008).
- [13] T. Igari, T. Fukahori, F. Kawashima, T. Tokiyoshi, Y. Chuman, N. Komai, M. Fujita, "Micro-macro creep damage simulation for welded joints", Materials at High Temperatures, Vol.28 No.3 (2011) 181-187. <http://dx.doi.org/10.3184/096034011X13123545763673>.
- [14] ST. Tu, P. Segle and JM. Gong, "Creep damage and fracture of weldments at high temperature", Int. J. Pressure Vessels and Piping, Vol.81, Issue 2 (2004) 199-209.
<https://doi.org/10.1016/j.ijpvp.2003.11.010>.
- [15] TH. Hyde, W. Sun and JA.Williams, "Creep analysis of pressurized circumferential pipe weldments - A review", J Strain Analysis, Vol.38, No.1, pp.1-29 (2004).
<https://doi.org/10.1115/PVP2016-63355>.
- [16] M. Yatomi, AD. Bettinson, NP. O'Dowd, KM. Nikbin, "Modelling of damage development and failure in notched - bar multiaxial creep tests", Fatigue & Fracture of Engineering Materials &

- Structures, Vol.27 (2004) 283-295. <https://doi.org/10.1111/j.1460-2695.2004.00755.x>.
- [17] H. Hongo, M. Tabuchi, Y. Li, Y. Takahashi, “Creep damage behavior of Mod.9Cr-1Mo steel welded joint”, J. The Japan Society of Materials Science, Japan, Vol.58, No.2 (2009) 101-107. <https://doi.org/10.2472/jsms.58.101>.
- [18] T. Fukahori, T. Tokiyoshi, T. Igari, Y. Chuman, M. Fujita and F. Kawashima, “Microscopic simulation and life prediction of high Cr steel welds subject to Type IV creep damage”, J. The Japan Society of Materials Science, Japan, Vol.62, No.2 (2013) 82-87. <https://doi.org/10.2472/jsms.62.82>.
- [19] T. Fukahori, T. Tokiyoshi, T. Igari, Y. Chuman and N. Komai, “Prediction of Type-IV creep failure of a seam-welded mod. 9Cr-1Mo elbow based on microscopic damage simulation”, Materials at High Temperatures, Vol.34, Issue 3 (2017) 194-207. <https://doi.org/10.1080/09603409.2017.1289621>.
- [20] T. Honda, T. Fukahori, T. Igari, Y. Chuman, T. Tokiyoshi and ACF. Cocks, “Creep damage analysis of simulated-HAZ notched bar specimens of modified 9Cr-1Mo steel”, JSME Mechanical Engineering Journal, Vol. 4, No. 5 (2017) 1-13. <https://doi.org/10.1299/mej.16-00697>.
- [21] Gonzalez, D., Cocks, A.C.F., Fukahori, T., Igari, T. and Chuman, Y., “Creep failure of a P91 simulated heat affected zone material under multiaxial state of stress”, Proc. 3rd Intern. ECCC Conf. on Creep & Fracture, (2014).
- [22] IJ. Perrin, and DR. Hayhurst, “Continuum damage mechanics analyses of type IV creep failure in ferritic steel crossweld specimens”, Int. J. Pres. Ves. Pip., Vol.76, Issue 9 (1999) 599-617. [https://doi.org/10.1016/S0308-0161\(99\)00051-4](https://doi.org/10.1016/S0308-0161(99)00051-4).
- [23] Dyson, B., “Continuous cavity nucleation and creep fracture”, Scripta Metallurgica, Vol. 17 (1983), pp. 31-37.
- [24] M. Fujimoto, M. Sakane, S. Date, H. Yoshida, “Multiaxial creep rupture and damage evaluation for 2.25Cr-1Mo forged steel”, J. Soc. Mat. Sci., Japan, Vol.54, No.2 (2005), pp.149-154. <https://doi.org/10.2472/jsms.54.149>.
- [25] Lemaitre J., “A continuum damage mechanics model for ductile fracture”, Trans ASME J. Eng. Mater. Technol. Vol.107(1985), pp.83–89. <https://doi.org/10.1115/1.3225775>.
- [26] K. Kimura and Y. Takahashi, “Evaluation of long-term creep strength of ASME Grades 91, 92, and 122 Types steels”, Proceedings of ASME 2012 Pressure Vessels and Piping conference, Toronto, Ontario, Canada, PVP2012- 78323(2012). <https://doi.org/10.1115/PVP2012-78323>.
- [27] K. Kimura and M. Yaguchi, "Re-evaluation of long-term creep strength of base metal of ASMIE grade 91 type steel", Proc. ASME PVP 2016, Vancouver, Canada, PVP 2016 -63355 (2016). <https://doi.org/10.1115/PVP2016-63355>.
- [28] K. Arisue, N. Komai, K. Tominaga, M. Fujita, “Relationship of long-term creep rupture strength between base metal and weldment in mod. 9Cr-1Mo steels”, Proc. Joint EPRI-123HiMAT Int. Conf.

on Advances in High Temp. Materials, Nagasaki (2019).

- [29] The Japan Society of Mechanical Engineers, Code for Nuclear Power Generation Facilities, Rules on Design and Construction for Nuclear Power Plants, Section II Fast Reactor Standards (2012)
- [30] S. Nishinoiri, Y. Takahashi, H. Fukutomi and M. Yaguchi, "Inner pressure/bending creep test on circumferentially welded large diameter pipe of Grade 91 steel: Creep Damage Mechanism and Applicability of NDE", Proc. ASME PVP2016, Vancouver, Canada, PVP2016-63176 (2016).
<https://doi.org/10.1115/PVP2016-63176>.
- [31] S. Matsuoka, "Relation between 0.2% proof stress and Vickers hardness and work-hardened low carbon-austenitic stainless steel, SUS316", Trans. JSME, Vol.70, N0.698A (2004) pp.1535-1541.
<https://doi.org/10.1299/kikaia.70.1535>
- [32] Y. Hasegawa, T. Muraki, M. Ohgami, "Identification and formation mechanism of a deformation process determining microstructure of Type IV creep damage of the advanced high Cr containing ferritic heat resistant steel", Tetsu- to-Hagane, Vol.90, No. 10, pp.609-617 (2004).
https://doi.org/10.2355/tetsutohagane1955.92.10_609.
- [33] K. Arisue, N. Komai, K. Tominaga, M. Fujita, "Long-term creep rupture strength and microstructural evolution for weldment in mod.9Cr-1Mo steels", Research Report for 123rd Committee on Heat-Resisting Materials and Alloys, Japan Society for the Promotion of Science (2016).
- [34] Y. Takahashi, S. Nishinoiri and M. Yamaguchi, " Development of analytical evaluation methods for creep failure in weldments of high chromium steels and application to full scale pipe experiments", Proceedings of ASME 2016 Pressure Vessels and Piping conference, Vancouver, Canada, PVP 2016 -63834 (2016). <https://doi.org/10.1115/PVP2016-63834>.
- [35] T. Honda, T. Fukahori, T. Tokiyoshi, Y. Chuman, T. Igari, "Creep damage analysis of large-size uniaxial cross weld specimen and circumferentially welded pipe of mod. 9Cr-1Mo steel", J. The Japan Society of Materials Science, Japan, Vol.68, No.2, pp.99-105 (2019).
<https://doi.org/10.2472/jsms.68.99>.

- A new approach to damage evaluation for Type IV creep failure at high temperatures.
- Creep damage in welded joints of modified 9Cr-1Mo steel is focused.
- Number density of creep void in FGHAZ is considered in damage mechanics approach.
- Creep crack initiation and propagation in welded joints are simulated.
- Simulated results are compared with experimental results.

Declaration of interests

☒ The authors declare that they have no known competing financial interests or personal relationships that could have appeared to influence the work reported in this paper.

☐ The authors declare the following financial interests/personal relationships which may be considered as potential competing interests: